Sustainability of apparent slip in micro-channel flows

Raghuraman N. GOVARDHAN[*,1], Pradeep S. PAWAR[1] & Musuvathi S. BOBJI[1],

* Corresponding author: Tel.: ++91 (0) 80 2292 3232; Fax: ++91 (0) 80 2360 0648; Email: raghu@mecheng.iisc.ernet.in
[1]Department of Mechanical Engineering, Indian Institute of Science, Bangalore – 560 032, INDIA

Abstract In the present work, we experimentally study the flow of water over textured hydrophobic surfaces in a micro-channel. Shear stress measurements are done along with direct visualization of trapped air pockets on the hydrophobic surface. The trapped air pockets on such surfaces are known to be responsible for apparent slip at these surfaces and hence in significant drag reduction. In typical circumstances, the apparent slip reduces over time as seen, for example, from our shear stress measurements. This implies that the drag reduction will not be sustained. We have performed extensive visualizations of the trapped air pockets while varying flow parameters like the flow rate and the pressure. We present here direct visualizations that show that under some conditions, the air pockets can grow with time. The variation of the air pocket size with time is found to change qualitatively and quantitatively as the flow rate is varied. These measured changes in the air pocket size with time have a direct bearing on the sustainability of apparent slip in micro-channel flows.

Keywords: Hydrophobic surface, Apparent slip, Drag reduction, Air pockets

1. Introduction

The flow of water over textured hydrophobic or superhydrophobic surfaces has been recently studied by a number of investigators (Watanabe et al., 1999; Tretheway & Meinhart, 2002; Choi et al., 2003; Ou et al., 2004; Truesdell et al., 2006) due to the possibility of substantial drag reduction in micro-channels composed of such surfaces. These large drag reductions are thought to be caused by the air trapped within the cavities of the superhydrophobic surface that in effect presents a composite solid-air interface to the flowing water. The flow over such a surface may thus be modeled of as consisting of regions of "no-slip", representing flow over the solid surface, and of "perfect slip" representing the parts where the water is in contact with the air (Lauga & Stone, 2003). Macroscopically this would give rise to an "apparent slip" that can be measured for the flow over the composite surface. A commonly used measure for slip is the apparent slip length (β) defined as the ratio of slip velocity to the velocity gradient at the surface.

Recent studies have shown that although apparent slip and large drag reductions can be obtained, sustaining them over larger periods of time is an issue. Govardhan et al. (2009) have shown that the apparent slip reduces with time as the air diffuses out of the air pockets on the textured hydrophobic surface. Bobji et al. (2009) have also directly visualized the air pockets on different types of textured hydrophobic surfaces and shown the loss of the "Cassie state" with time. These studies show that the sustainability of apparent slip is an important issue for obtaining long-term drag reduction in hydrophobic micro-channels.

In the present work, we study the flow through a high-aspect ratio micro-channel whose one wall is made using a textured hydrophobic surface. Shear stress measurements and direct visualization of the trapped air pockets on the textured hydrophobic surface have been done. Detailed measurements of the variations with time of the trapped air pockets under different flow

conditions in the micro-channel are presented in this paper.

2. Experimental methods

A schematic of the basic experimental arrangement is shown in figure 1. One wall of a large aspect ratio micro-channel is made of a superhydrophobic surface, while the remaining walls are hydrophilic. The shear stress on the wall containing the hydrophobic surface can be measured by a movable sensing area mounted on a double cantilever arrangement. The deflection of the sensing area in the streamwise direction is proportional to the shear stress. The very small streamwise deflections of the sensing area, of the order of 20 microns, is measured using a sensitive optical reflectance based fiber optic displacement transducer with a resolution of better than 0.2 microns.

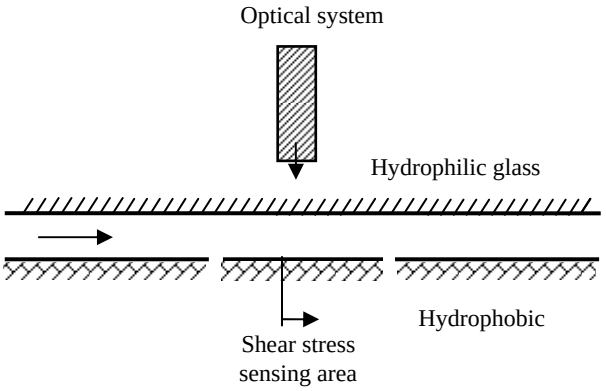

Figure 1. Schematic of the experimental arrangement showing flow through a high aspect ratio micro-channel. One wall of the micro-channel is made using a hydophobic surface and the shear stress on this can be measured using a sensing area that can deflect in the streamwise direction.

The trapped air pockets on the surface can be directly visualized using a high magnification optical system from Navitar connected to high resolution Nikon digital SLR camera. This enables direct visualization of trapped air pockets that are of the order of 100 microns. From these direct visualizations of the trapped air pockets, measurements are made of their size as a function of time.

The hydrophobic surfaces used in the present work have physical features that are either irregular, as shown in figure 2, or a regular pattern, as shown in figure 3. The irregular surface was made by electrodischarge machining process and then coated with 1H,1H,2H,2H-perfluoro-octyl trichlorosilane (FOTS) to make it hydrophobic. The regular patterned surface was composed of holes made by chemical etching using a mask and then rendered hydrophobic using a coating of 1-dodecanethiol. The different chemical coatings were necessitated in the two cases because of the different materials used; aluminium in the first case, and brass in the second case. The holes on the regular surface had a diameter of about 100 microns with a pitch of 80 microns, and a depth of about 60 microns.

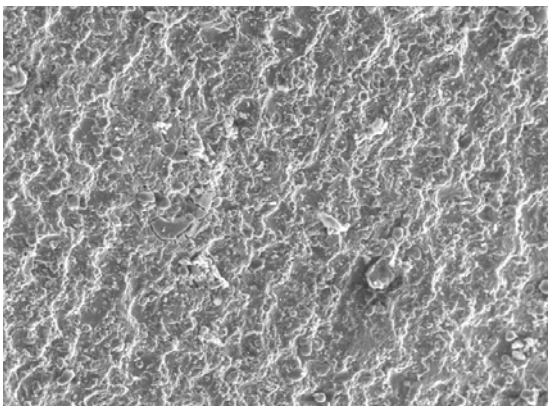

Figure 2. Scanning electron microscopy (SEM) image of a hydrophobic surface with irregular features of the order of 50 microns. The field of view in the image shown is about 1mm.

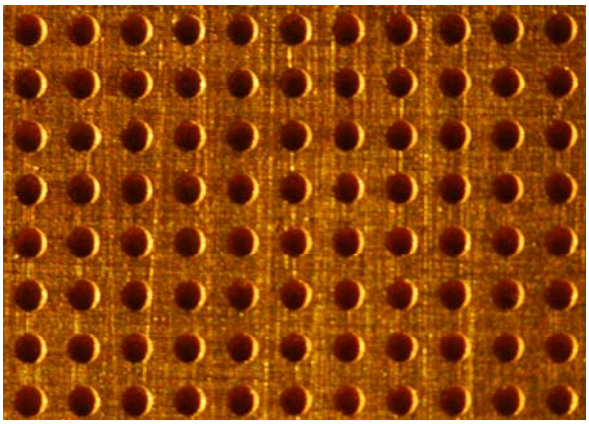

Figure 3. Optical micrograph of a regular patterned hydrophobic surface composed of holes of 100 microns diameter with a pitch of 80 microns.

3. Results

3.1 Irregular hydrophobic surface

We begin by presenting results of shear force measurements on the irregular hydrophobic surface shown in figure 2. For this, experiments were conducted at different times after initial submergence of the channel walls with water, and the apparent slip lengths were calculated as discussed in Govardhan et al. (2009) using the shear force measurements. The apparent slip lengths measured as a function of time are shown in figure 4. The first point to be noted is that the apparent slip length varies considerably with time. It can be seen that initially the slip length is large of the order of 50 microns, but then gradually reduces with time. After a few hours, the slip length tends to zero, indicating that there is "no-slip". This large reduction of the slip length with time may be attributed to the diffusion of air from the air pockets trapped in the crevices of the textured hydrophobic surface. This would result in the loss or reduction of the air that was in contact with the water that was primarily responsible for apparent slip and the consequent drag reduction.

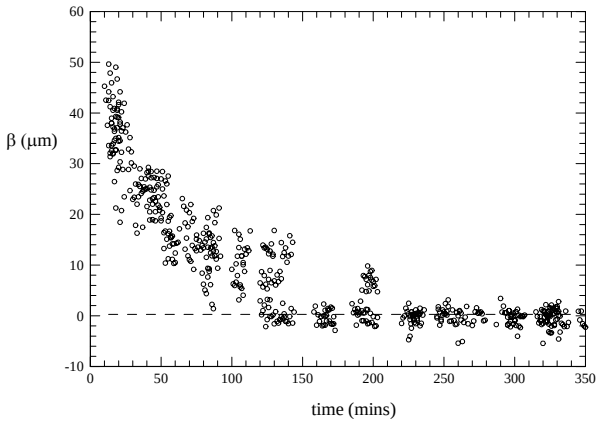

Figure 4. Variation of the apparent slip length (β) with time. The data shown here is obtained from the shear stress measurements at different times.

The above results show that sustaining the air pockets or bubbles on the surface of the hydrophobic surface are crucial to obtain long term drag reduction. Hence, we moved our attention to regularly patterned surface with holes, as shown in figure 3, to enable us to directly visualize the trapped air pocket or bubble on each hole.

3.2 Regular hydrophobic surface

In this section, we present results from experiments with regularly patterned hydrophobic surface shown in figure 3. Micro-channels with one wall composed of such a surface were used, and flow parameters such as the pressure within the channel and the flow rate through it were systematically varied. We present here direct visualization of the trapped air pocket or bubbles on the surface for the case corresponding to a pressure of 92.5 kPa, where the bubbles were seen to grow with time. The details of the bubble growth with time were measured and are presented below.

Figure 5 shows a time sequence of the zoomed in view of the air pocket or bubble corresponding to a single hole on the patterned surface. In each of the images shown, the inner circle corresponds to the physical hole. The air pocket or bubble corresponding to the hole is typically larger than the physical hole. The outer circle, in each image, corresponds to the interface between the bubble and the water in the channel. It is clear from the images that the bubble grows with time. In the first five images shown the bubble continuously increases in size, and then the bubble size suddenly decreases. This is due to detachment of the large bubble caused by the flow, leaving a relatively smaller bubble in its place. This cycle of bubble growth and detachment continues periodically. It may however be noted that there are cycle to cycle variations in the bubble growth time, and in the bubble size at detachment, as will be shown later.

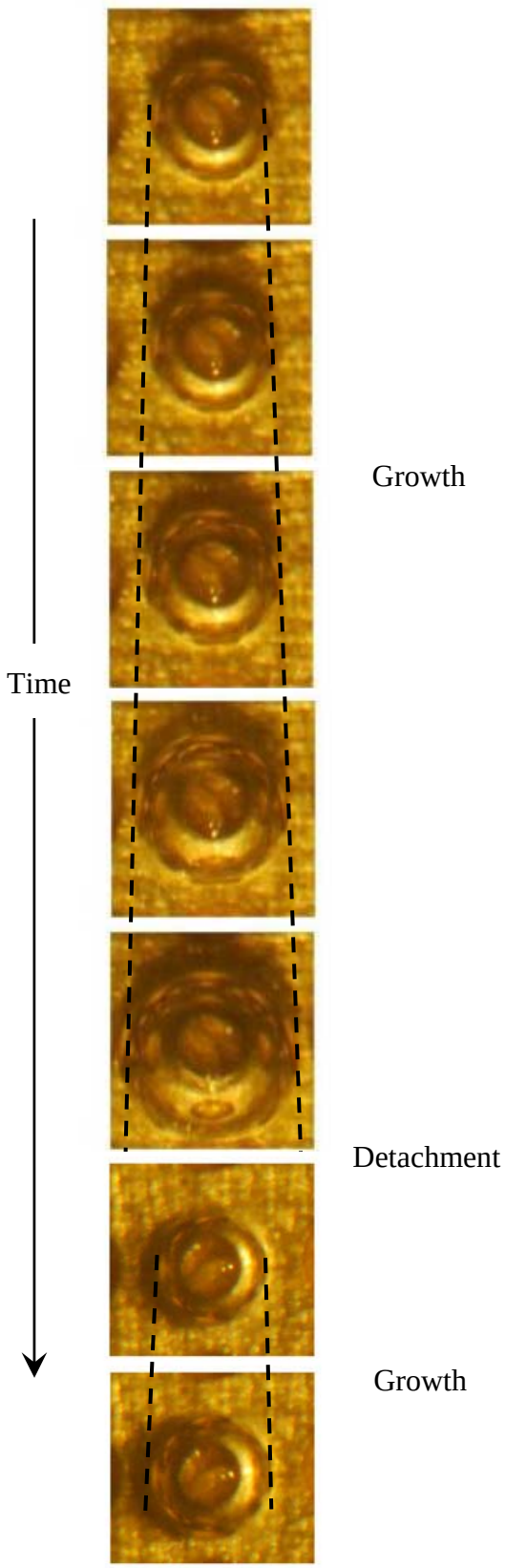

Figure 5. Time sequence of the zoomed in view of the air pocket or bubble corresponding to a single hole on the regularly textured surface. The bubble can be seen to grow, detach and then grow again.

The growth and detachment of the air bubble or pocket on the hydrophobic surface is found to vary with flow rate both qualitatively and quantitatively. We present in figures 6 and 7 a sequence of images corresponding to a low flow rate and a high flow rate case to first show the qualitative difference between the two cases. In both cases, we present results with a field of view of 8 holes to illustrate the differences.

The low flow rate case shown in figure 6 shows bubble growth with time for each hole. In addition to this bubble growth, merger of adjacent bubbles is also seen to take place in this case. In the images, the interface of the bubble is marked, in some cases, to highlight bubble growth and merger. For example, in figure 6(a), the marked bubble on the top right is growing and this leads to the merger of two vertically adjacent bubbles, as shown in figure 6(b). After this merger the bigger bubble in figure 6(b) now covers two holes, and the distorted view of the holes because of refraction of light through air may be seen. Subsequently, the bubble grows further and also merges horizontally covering 4 physical holes, as seen in figure 6 (c). This large bubble further grows with time before it detaches leaving 4 small air bubbles; one corresponding to each of the 4 holes. This cycle of bubble growth, followed by mergers, and detachment again repeats in a cyclical manner.

We present in figure 7 the high flow rate case with all other things remaining the same as in figure 6. It is clear that all the bubbles grow with time in this case as well. However, bubble mergers do not occur for this case. The bubbles grow and detach before there is any merger of adjacent bubbles. The interface corresponding one of the bubbles is highlighted in the figure to clearly show the difference with the lower flow rate case in figure 6. It may be noted that this qualitative difference is dependent on many factors including importantly the spacing between the holes on the surface.

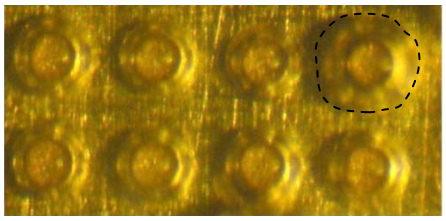

(a)

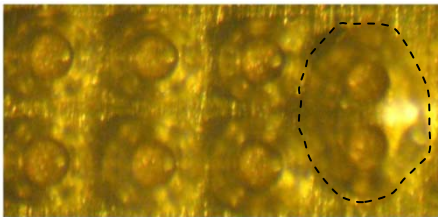

(b)

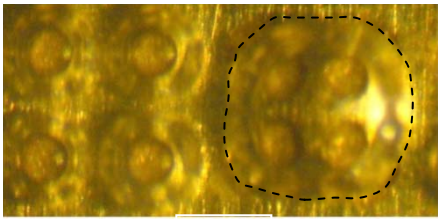

(c)

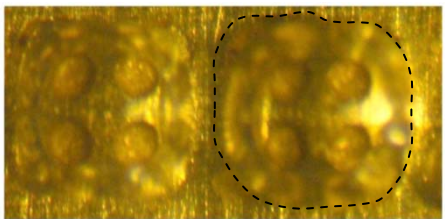

(d)

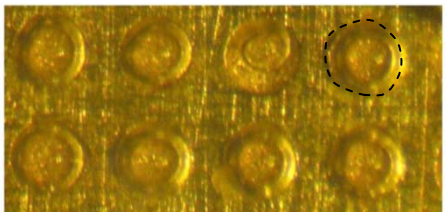

(e)

Figure 6. Time sequence of the air pocket or bubble on the regularly textured surface at low flow rate. The bubble can be seen to grow, merge in both vertical and horizontal directions, followed by detachment. The flow rate in this case is 9 ml/sec and the time corresponding to each image is (a) 0, (b) 130, (c) 180, (d) 220 and (e) 440 secs.

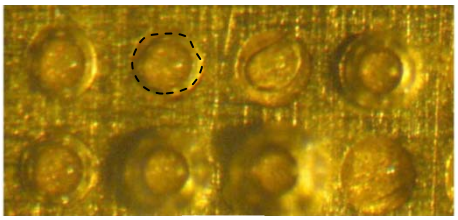

(a)

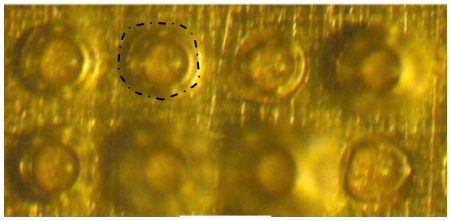

(b)

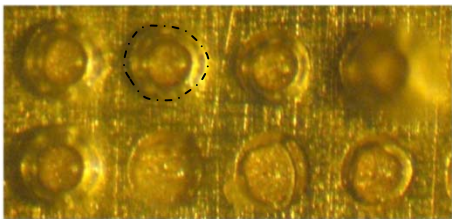

(c)

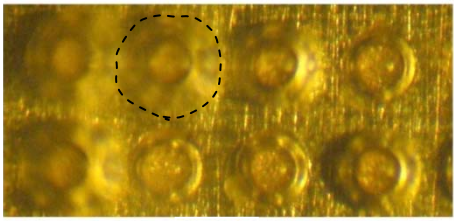

(d)

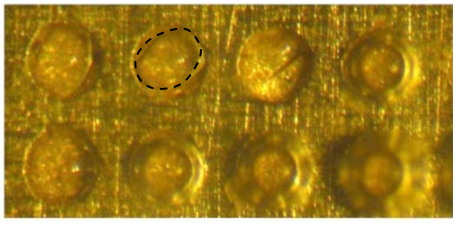

(e)

Figure 7. Time sequence of the air pocket or bubble on the regularly textured surface at high flow rate. The bubble can be seen to grow and then detach without merger with adjacent bubbles. The flow rate in this case is 15 ml/sec and the time corresponding to each image is (a) 0, (b) 35, (c) 55, (d) 135 and (e) 160 secs.

The qualitative behavior of bubble growth seen in figure 6 and 7 may be made more quantitative by obtaining, for example, the maximum bubble size (d) in the vertical direction as a function of time from the images. This is presented in figure 8 and 9 for the low and high flow rate cases. In each case, the bubble size is normalized by the size of the hole (d_o = 100 microns). In the low flow rate case, in figure 8, the bubble size grows gradually followed by a sudden increase corresponding to merger and then a sudden decrease corresponding to detachment of the bubble. The cycle repeats itself, although as seen in the figure, there are some cycle to cycle variations in the period. In the high flow rate case, shown in figure 9, the bubble grows and detaches without merger and this leads to much smaller bubble sizes, as one may expect. The period of the complete cycle is also substantially smaller in this case.

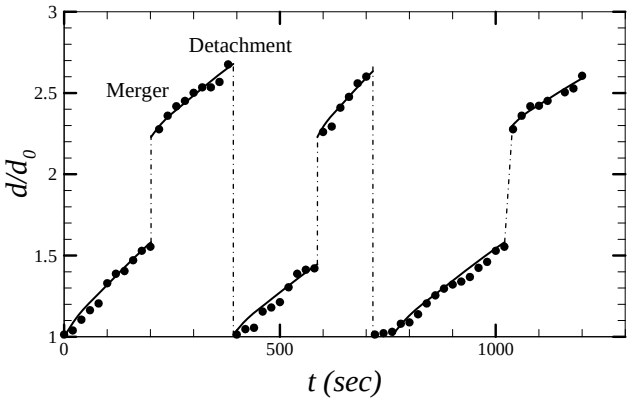

Figure 8. Variation of the normalized bubble size (d/d_o) with time for the low flow rate case corresponding to figure 5. Here, there is bubble growth, merger and subsequent detachment. The flow rate in this case is 9 ml/sec. do is the size of the hole (100 microns).

The bubble size as function of time for a single cycle is plotted in figure 10 for a few flow rates. This figure highlights the fact that there are considerable changes in the size of the bubble at detachment and the period for the bubble growth-merger-detachment cycle. The detachment of the bubble is particular is decided primarily by the drag force on the bubble overcoming the surface tension related force. It is easy to see that as the flow rate is increased, the drag would considerably increase leading to detachment of the bubble at smaller bubble sizes as observed in the experiments.

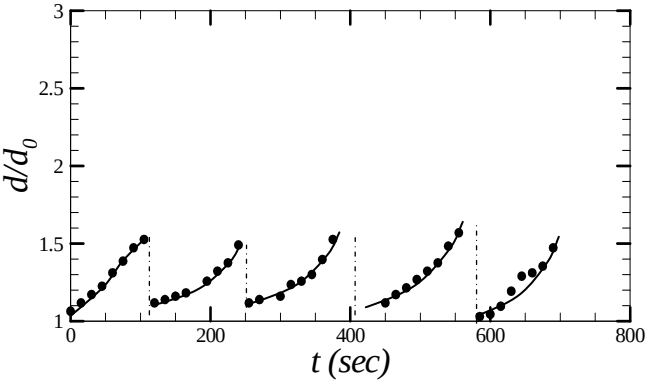

Figure 9. Variation of the normalized bubble size (d/d_o) with time for the high flow rate case corresponding to figure 6. Here, there is bubble growth, and subsequent detachment without merger. The flow rate in this case is 15 ml/sec.

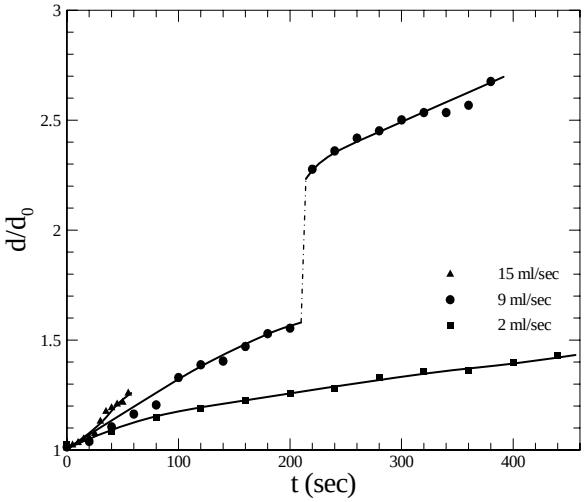

Figure 10. Variation of the normalized bubble size (d/d_o) with time for one cycle at a few flow rates. The growth rate of the bubble, as well as the diameter of the bubble at detachment, vary with the flow rate.

4. Discussion

The direct observation of growing bubbles on regularly patterned hydrophobic surfaces under flow conditions are interesting from the point of sustaining apparent slip over long times. This in turn has direct implications for sustained drag reductions in micro-channels using such hydrophobic surfaces.

It is also important to understand the qualitative and quantitative variations of the bubble size with time presented here. This would help to design better textures for such hydrophobic surfaces, so as to maximize the apparent slip and minimize the drag. Work is presently ongoing on a number of related issues and will be presented at the conference.

References

M.S. Bobji, Vijay Kumar S., A. Asthana, R.N. Govardhan, "Underwater Sustainability of the "Cassie" State of wetting," Langmuir 25(20), 12120–12126 (2009).

C. Choi, K.J.A. Westin, and K.S. Breuer, "Apparent slip flows in hydrophilic and hydrophobic microchannels," Phys. Fluids **15**, 2897 (2003).

R.N. Govardhan, G.S. Srinivas, A. Asthana and M.S. Bobji, "Time dependence of effective slip on textured hydrophobic surfaces," Phys. Fluids **21**, 052001 (2009).

E. Lauga and H.A. Stone, "Effective slip in pressure-driven Stokes flow," J. Fluid Mech. **489**, 55 (2003).

J. Ou, B. Perot, and J.P. Rothstein, "Laminar drag reduction in microchannels using ultrahydrophobic surfaces," Phys. Fluids **16**, 4635 (2004).

D. C. Tretheway and C. D. Meinhart, ''Apparent fluid slip at hydrophobic microchannel walls,'' Phys. Fluids **14**, L9 (2002).

R. Truesdell, A. Mammoli, P. Vorobieff, F. van Swol, and C.J. Brinker, "Drag reduction on a patterned superhydrophobic surface," Phys. Rev. Lett. **97**, 044504 (2006).

K. Watanabe, Y. Udagawa & H. Udagawa, "Drag reduction of Newtonian fluid in a circular pipe with a highly water-repellent wall," J. Fluid Mech. **381**, 225 (1999).